Electric field-modulated amplified spontaneous emission in organo-lead halide perovskite CH3NH3PbI3

Article *in* Applied Physics Letters · December 2015

DOI: 10.1063/1.4938754

CITATION
1

READS
60

8 authors, including:

Zhaoxin Wu
Xi'an Jiaotong University
114 PUBLICATIONS **981** CITATIONS
SEE PROFILE

Hua Dong
Xi'an Jiaotong University
35 PUBLICATIONS **129** CITATIONS
SEE PROFILE

Jun Xi
Xi'an Jiaotong University
17 PUBLICATIONS **46** CITATIONS
SEE PROFILE

Xun Hou
Xi'an Jiaotong University
377 PUBLICATIONS **2,244** CITATIONS
SEE PROFILE

AIP | Applied Physics Letters

Electric field-modulated amplified spontaneous emission in organo-lead halide perovskite CH3NH3PbI3

Fang Yuan, Zhaoxin Wu, Hua Dong, Bin Xia, Jun Xi, Shuya Ning, Lin Ma, and Xun Hou

Citation: Applied Physics Letters **107**, 261106 (2015); doi: 10.1063/1.4938754
View online: http://dx.doi.org/10.1063/1.4938754
View Table of Contents: http://scitation.aip.org/content/aip/journal/apl/107/26?ver=pdfcov
Published by the AIP Publishing

Electric field-modulated amplified spontaneous emission in organo-lead halide perovskite $CH_3NH_3PbI_3$

Fang Yuan,[a] Zhaoxin Wu,[a),b)] Hua Dong, Bin Xia, Jun Xi, Shuya Ning, Lin Ma, and Xun Hou
Key Laboratory of Photonics Technology for Information, Department of Electronic Science and Technology, School of Electronic and Information Engineering, Xi'an Jiaotong University, Xi'an 710049, People's Republic of China

(Received 24 July 2015; accepted 13 December 2015; published online 29 December 2015)

The electric field-modulation of the spontaneous emission (SE) and amplified spontaneous emission (ASE) in organo-lead halide perovskite $CH_3NH_3PbI_3$ (aliased as $MAPbI_3$) layer has been investigated. With the increase of the external applied electric field, the electric field-induced quenching of the SE and ASE intensity was observed, accompanying with a blue-shift of the ASE emission peaks, which can be attributed to field-induced ionization of photogenerated excitons in the $MAPbI_3$ layer. Based on the analysis of quenching factor and the dielectric constant, we estimated an exciton binding energy ~36 meV at room temperature, which will provide useful insights into the optical-electrical characteristics of $MAPbI_3$ and pave the way for the future optoelectronic applications. © *2015 AIP Publishing LLC*. [http://dx.doi.org/10.1063/1.4938754]

Recently, organo-lead halide perovskites have attracted extensive attention due to their excellent power conversion efficiency as light absorbers of solar cells, which have continuously been promoted up to as high as 20.1% lately.[1,2] Interestingly, the observation of high quantum yield photoluminescence (PL) and optical gain in solution-processed hybrid perovskites with different halides also makes these materials promising candidate for light emitting diodes and low-cost on-chip coherent light sources that can be easily tuned across the entire visible spectrum.[3–7]

Given the rapid rise in performance of perovskite photovoltaic devices and their applications in light-emitting diodes, exploring the optical properties of these materials is becoming an important issue. Numerous studies, which focused on the optical absorbance, excitonic properties, and recombination lifetimes, have been made to investigate the specific material properties in the perovskite films, revealing the optoelectronic processes accompanied with established theoretical models.[8–13] Among them, an important question that whether the excited states in the $MAPbI_3$ layer is mainly composed of free or bound charge carriers depending on the exciton binding energy E_b has been a matter of intense debate. Therefore, the values for E_b of $MAPbI_3$ have been extensively investigated. Based on a variety of methods, such as optical absorption, temperature dependent PL, and magnetoabsorption, some studies estimated the values for E_b ranging from 19 to 50 meV, which are comparable with the thermal kinetic energy of ~26 meV at room temperature, declaring the coexistence of free carriers and excitons.[14–17] The others concluded the values for E_b much smaller than 26 meV, indicating a non-excitonic mechanism.[9,18–20] Generally speaking, the value of E_b for Wannier exciton in $MAPbI_3$ has yet to be further confirmed.

In addition, electromodulation of PL, which can provide valuable information on the exciton formation, carrier generation, recombination, and ionization of excitons in the presence of external electric field, has been increasingly applied in the research of semiconductors.[21–24] However, little research has been done on electric field-modulation of ASE in organo-lead halide perovskite $MAPbI_3$ so far, which in fact can offer lots of interesting information about their optoelectric characteristics.

In this letter, we report the electric field-modulation of spontaneous emission (SE) and ASE in the optically pumped $MAPbI_3$ layer. The electric field quenching of the SE and ASE was observed with the increase of the external electric field, which can be attributed to field-induced ionization of photogenerated excitons in the $MAPbI_3$ layer. From the electric field dependence of quenching factor, the exciton binding energy was estimated as 36 meV, which will provide insights into the characteristics of the excited states in $MAPbI_3$.

The sample was fabricated on an indium-tin oxide (ITO)-coated patterned glass substrate. The polyvinyl alcohol (PVA) aqueous solution and polymethylmethacrylate (PMMA) dissolved in chlorobenzene solution were spin-coated onto the substrate as the insulating layers. The $MAPbI_3$ layer was prepared as follows: Lead iodide (PbI_2, Sigma-Aldrich) about 120 nm was deposited onto the PVA coated substrate via thermal evaporation. Then, the substrate was soaked in isopropyl alcohol solution of CH_3NH_3I (10 mg/ml) for 60 s in N_2 ambient glove box to form the perovskite layer. Finally, LiF and Ag film were successively deposited onto the substrate to complete the device, with the structure of Glass/ITO/PVA/$MAPbI_3$/PMMA/LiF/Ag, as shown in Fig. 1(a). The scanning electron micrograph (SEM) of $MAPbI_3$ layer is presented in Fig. 1(b). The as-formed $MAPbI_3$ layer possesses the characteristics of full surface coverage on the substrate, with distinct grain size of about 130–165 nm. The thickness measured by ellipsometry of PVA, $MAPbI_3$, PMMA, LiF, and Ag film is 315 ± 15 nm,

[a)]F. Yuan and Z. Wu contributed equally to this work.
[b)]Author to whom correspondence should be addressed. Electronic mail: zhaoxinwu@mail.xjtu.edu.cn

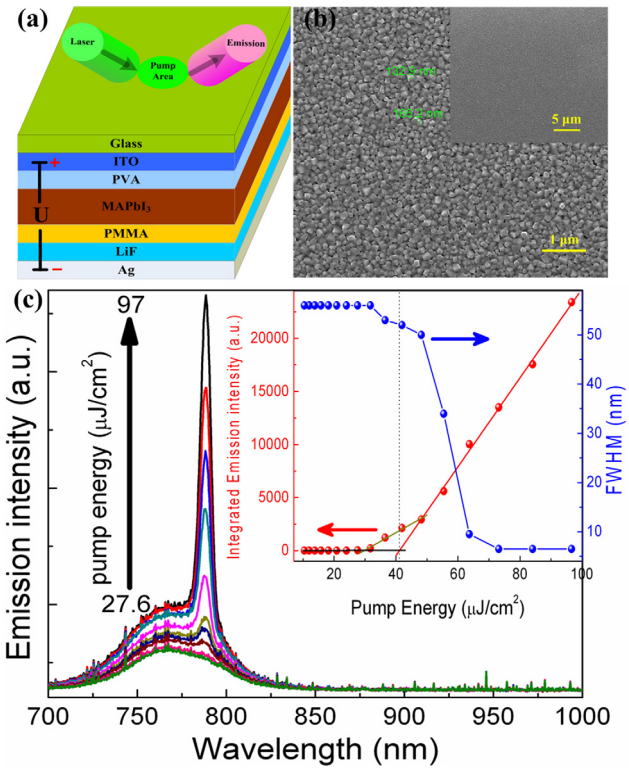

FIG. 1. (a) Schematic configuration of the sample. (b) Top view SEM image of the $MAPbI_3$ layer. (c) Face emission spectra of the sample plotted as a function of pump energy. The insets show the integrated emission intensity and the FWHM of the face emission spectra as a function of pump energy.

240 ± 30 nm, 85 ± 10 nm, 250 nm, and 140 nm, respectively. All measurements were carried out under ambient environment at room temperature.

The sample was excited at 532 nm by a frequency-doubled Nd:YAG laser delivering 5 ns pulses at a 10 Hz repetition rate. Through a pinhole filter and a positive lens, the laser beam formed a 3 mm diameter spot, and was irradiated obliquely onto the surface of the samples with the ITO area of $3\,\text{mm} \times 3\,\text{mm}$. Face emission spectra were collected directly into Fiber Optic Spectrometer. The measured output emission spectra, input-output intensity, and the full width at half maximum (FWHM) FWHM as a function of increasing pump energy are shown in Fig. 1(c). At low pump energy, only an SE peak at 766 nm with the FWHM about 56 nm is observed. When the pump intensity exceeds the threshold, the spectral narrowing, i.e., ASE, emerges at 788 nm while the FWHM dramatically decreased to about 6.5 nm at 75 $\mu J/cm^2$. To further improve the pump energy, the FWHM remains constant. Clearly, as shown in the inset of Fig. 1(c), there is an obvious threshold about 41 ± 5 $\mu J/cm^2$ in the input-output curve. The reason that ASE can be achieved in the $MAPbI_3$ layer is that the spontaneously emitted photons transmitted along gain media are amplified by stimulated emission. Owing to the stronger self-absorption, ASE does not occur at the SE peak wavelength 766 nm but at 788 nm where the optical gain and absorption are balanced.[4] It is worth mentioning that the ASE peak wavelength of the sample does not shift as the pump energy increases.

In order to further investigate the mechanisms of exciton photogeneration, recombination, and ionization in $MAPbI_3$, the emission spectra excited at the identical pump intensity 97 $\mu J/cm^2$ under different direct current (DC) voltages using a DC power supply was obtained as shown in Fig. 2(a) clearly. The average static applied electric field F is calculated using $F = V/d$, where V is the voltage on the device and d the total thickness between the electrodes. By the way, the insulating layers between the two electrodes were thick enough to prevent electrons and holes from injecting into the active $MAPbI_3$ layer. As shown in Fig. 2(b), both the SE and ASE intensities remain almost constant first under appropriate electric field ($\sim 10^5$ V/cm), then decrease with further increasing applied voltage. Meanwhile, the ASE emission peaks remain constant as 788 nm first smaller than 10^5 V/cm, then blue-shift to 782 nm with further increasing applied electric field whereas the SE emission peaks remain unchanged at 766 nm. Interestingly, the electric field-induced ASE intensity quenching is dramatically aggrandized in accompany with the blue-shift of ASE emission wavelength at the same electric field range.

To comprehensively understand the quenching mechanisms of the SE and ASE in $MAPbI_3$ with electric field, we should get to know the fact that the SE and ASE of $MAPbI_3$ originate from whether excitons or free carriers under the photoexcitation. As we know, with the increasing excitation intensity in semiconductors, the more formed excitons will lose their identity as individual quasiparticles and produce the electron-hole plasma (EHP). The transition from the exciton gas to EHP generally occurs at the density of

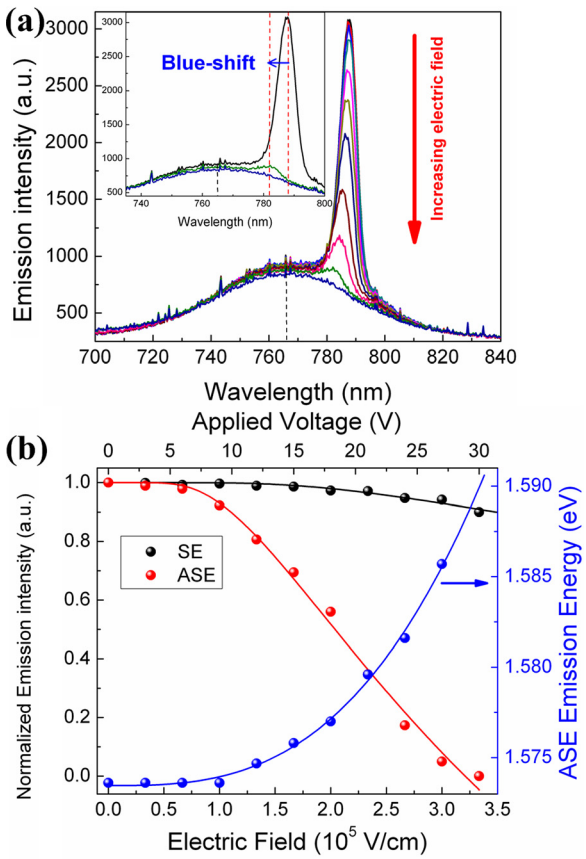

FIG. 2. (a) Face emission spectra at the identical pump intensity 97 $\mu J/cm^2$ under different DC voltages. (b) The electric field dependence on the SE (black curve) and ASE (red curve) normalized emission intensity and ASE emission wavelength under different electric fields or DC voltages (blue curve).

optically injected electron-hole pairs, Mott density n_M.[25] By considering an electron-hole gas described by classical Boltzmann statistics at room temperature, the Mott density can be calculated as $n_M = 1.19^2 k_B T/2a_B^3 E_b \sim 3\times10^{19}\,\mathrm{cm}^{-3}$, where k_BT is the thermal kinetic energy (~26 meV) at room temperature and a_B the effective Bohr radius for excitons in $MAPbI_3$. In addition, considering the larger dielectric constant ~18 derived from capacitance measurement for $MAPbI_3$,[26] the Mott density n_M is still larger than $10^{19}\,\mathrm{cm}^{-3}$. In our experiment, the density of optically injected electron–hole pair n in $MAPbI_3$ can be estimated by multiplying the laser pulse photon fluence times the film absorption coefficient, ranging from 10^{16} to $10^{19}\,\mathrm{cm}^{-3}$. Fig. 3 shows the integrated PL intensity and the emission quantum yield as a function of the injected carrier density. With the increase of the injected carrier density, the integrated PL intensity grows rapidly before showing some saturation at higher pump energy. Correspondingly, the emission quantum yield, calculated as the integrated PL intensity divided by the injected carrier density, grows linearly, then saturates, and for $n > 10^{18}\,\mathrm{cm}^{-3}$, it decreases due to gradually increasing nonradiative processes. The PL intensity tends to saturate higher than the threshold 44 μJ/cm^2, corresponding to an injected carrier density $n_{las} \sim 4.2\times10^{18}\,\mathrm{cm}^{-3}$. Obviously, n_{las} is much smaller than n_M, which means that the transition from excitonic gas to EHP has not emerged.

In addition, in our experiment, the sample was pumped by nanosecond pulsed laser. According to the previous reports, the lasing actions of $MAPbI_3$ layer occur in ten picoseconds period,[4] which means that lower lasing threshold could be obtained by femtosecond pulsed laser. In fact, Xing *et al.* reported the lower lasing threshold as 12 μJ/cm^2 with 150 fs laser pulse, and the recent reports show the extremely low threshold as 0.22 μJ/cm^2 for the $MAPbI_3$ nanowire, corresponding to n_{las} as low as $1.5\times10^{16}\,\mathrm{cm}^{-3}$, which is three orders lower than Mott density.[4,27] From this point, it is reasonable to consider that the Wannier excitons exist in $MAPbI_3$.

In fact, the net amplification cannot occur by single exciton recombination process but the multiexciton and/or scattering effects. As we know, for the direct gap semiconductor (GaN, ZnO, CdS, and others), the stimulated emission results from the inelastic excitonic scattering process in the intermediate density regime, such as exciton-exciton scattering.[28,29] Although the inelastic excitonic scattering process is a complicated process and beyond the scope of this paper, it does depend on the existence of the Wannier excitons, and the ionization of Wannier exciton is sure to reduce the excitonic scattering and interaction process, which is also sure to quench PL or ASE from the multiexciton and/or scattering effects. As the result, by studying the behavior of Wannier excitons under external electric field, we can explain the quenching and blue-shift of SE and ASE in $MAPbI_3$, which is discussed in detail later.

The quenching of the SE and ASE could be considered as the result of ionization of Wannier excitons photogenerated in $MAPbI_3$ at room temperature. The Coulomb potential of the electron-hole pair without and with an externally applied electric field is shown in the inset of Fig. 4. The primary effect of the electric field is to lower the lip of the potential well, which causes the bound levels to be mixed into a continuum. When the external electric field in a semiconductor is sufficiently high, a finite probability exists for interband quantum tunneling, i.e., direct transition of electrons from the conduction band into the valence band, or vice versa. As the result, the tunneling probability is proportional to the quenching of the ASE in $MAPbI_3$ under appropriate electric field. The tunneling probability T_t can be better described by a one-dimensional model for tunneling through a parabolic potential barrier[21,30]

$$T_t = A\exp\left(-\pi\sqrt{\mu}E_b^{3/2}/2\sqrt{2}\hbar eF\right), \tag{1}$$

where A is a free fit parameter, μ the effective mass, $\hbar$ the Planck constant, e the unit charge, and E_b the exciton binding energy. From the emission intensity measured in the presence and in the absence of electric field [$I(F)$ and $I(0)$, respectively], the quenching factor Q is introduced, which is

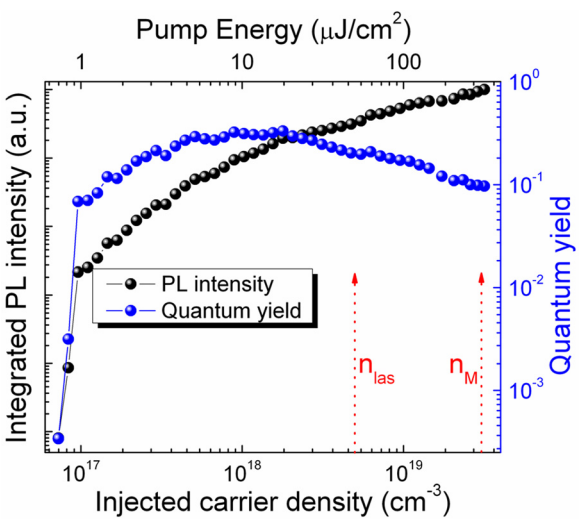

FIG. 3. The integrated PL intensity (black dots) and the emission quantum yield (blue dots) are plotted as a function of the injected carrier density and pump energy.

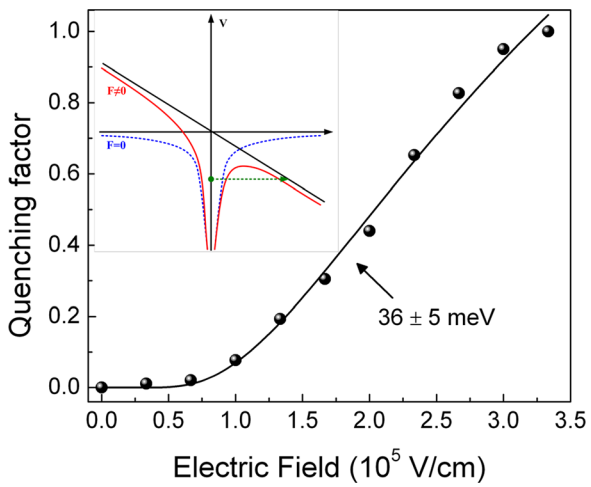

FIG. 4. The electric field dependence of quenching factor Q. The experimental values of quenching factor Q (dots) for ASE data and the ideal fit (line) of the data with Equation (2) yielded $E_b = 36 \pm 5$ meV. The inset shows the Coulomb potential of an exciton without and with an applied electric field.

proportional to ionization of excitons and tunneling probability, using[21,22,31,32]

$$Q = 1\text{–}I(F)/I(0) = T_t. \quad (2)$$

The quenching factor Q can be experimentally calculated according to Equation (2), which is shown in Fig. 4 as the dots. Considering the fact that Q is proportional to the tunneling probability, the electric field dependence of Q which can help identify the nature of the exciton is shown in Fig. 4 in solid line. The ideal fit of the data with Equation (2) yielded $E_b = 36 \pm 5$ meV for ASE data, which is similar to part of the previously reported values mentioned earlier. In addition, in order to further theoretically calculate E_b, we obtained the real part ε_1 and the imaginary part ε_2 of the complex dielectric constant for $MAPbI_3$ based on the capacitance measurement in very low frequency regime and the ellipsometry data in the optical frequency range. As apparent in Fig. 5, the dielectric constant ε for $MAPbI_3$ is frequency-dependent, which shows a static value ~13 at very low frequency and a lower value ~6 at optical frequency. A value for ε between these two values should be used to calculate the exciton binding energy for Wannier exciton by $E_b = \mu e^4/2\hbar^2\varepsilon^2$ if E_b is greater than the optical phonon energies.[25] For $MAPbI_3$, a value for $\varepsilon \sim 6$ was estimated to calculate E_b, corresponding to a value about 38 meV, which is comparable with our fitting value shown in Fig. 4. The electric field which is capable of ionizing excitons must provide at least a potential drop of one effective Rydberg energy across the effective Bohr radius a_B, i.e., the ionization field $F_{ion} = E_b/ea_B \sim 10^5$ V/cm, little less than the external applied electric field at the turning point as shown in Fig. 2(b). We deduce that the effective electric field on excitons is approximately overvalued on account of the built-in electric field formed inside the device when the applied electric field is homogeneous.[33]

It is very worth mentioning that much higher electric field leads to a blue-shift of ASE wavelength. According to the calculations by Blossey,[34,35] the exciton energy levels will shift to higher energies due to mixing with the continuum states at high electric field, which is consistent with our experimental results that a blue-shift about 13 meV of ASE emission peaks is observed at 3.4×10^5 V/cm. The originally bound exciton states become degenerate with the free continuum states at high electric field. The exciton is then no longer bound, and its energy levels correspond then to a maximum of its density of states. The blue-shift here follows an $(F/F_{ion})^{2/3}$ law, characteristic for the first oscillation peak of a simple band-to-band Franz-Keldysh effect.[36]

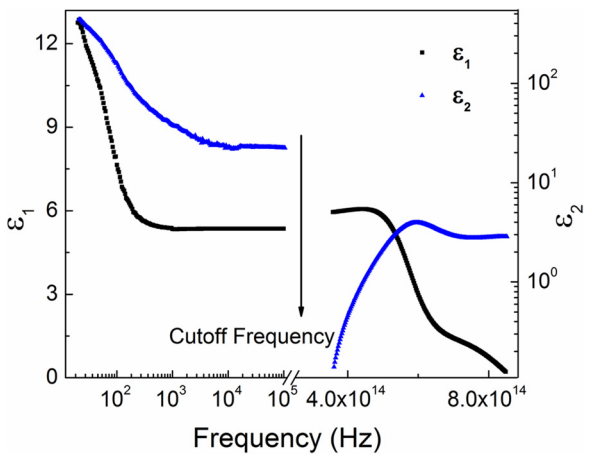

FIG. 5. Complex dielectric constant of the $MAPbI_3$ layer obtained from the capacitance measurement and the ellipsometry data: the real part ε_1 (black) and the imaginary part ε_2 (blue).

The above results imply that all the fluorescence emissions can be quenched by a strong electric field. When the electric field applied to $MAPbI_3$ is high enough, excitons will be ionized to form separate electrons and holes, which results in a decrease in fluorescence emission. As shown in Fig. 2(b), ASE quenching up to about 100% at the external electric field of 3.4×10^5 V/cm is observed, offering potential applications as electric field-modulated amplifiers and optical switches.[31]

In summary, we have investigated the electric-field modulation of the SE and ASE in $MAPbI_3$ film. The electric-field quenching of the SE and ASE was observed, accompanying with blue-shift of ASE emission peaks. We attributed the electric field dependence of the SE and ASE intensity to field-induced ionization of excitons in the $MAPbI_3$ layer. The ionization of excitons reduced the excitonic scattering and interaction process, which was considered to be responsible for ASE. By the fitting of the dependence of quenching factor on the electric field, an exciton binding energy of 36 meV at room temperature was yielded. Our results provide useful insights into the optical properties of the hybrid perovskite, promoting their future applications in optoelectronic devices.

This work was financially supported by Basic Research Program of China (2013CB328705), National Natural Science Foundation of China (Grant Nos. 11574248, 61275034), Ph.D. Programs Foundation of Ministry of Education of China (Grant No. 20130201110065), and International Cooperation by Shaanxi (Grant No. 2015 KW-008). We also appreciate Professor Xiaoyong Wei for his helpful discussions, and Dr. Peng Shi, Dr. Song Xia, and Dr. Fan He for the measurement of dielectric constant.

[1]A. Kojima, K. Teshima, Y. Shirai, and T. Miyasaka, J. Am. Chem. Soc. **131**, 6050 (2009).
[2]W. S. Yang, J. H. Noh, N. J. Jeon, Y. C. Kim, S. Ryu, J. Seo, and S. I. Seok, Science **348**, 1234 (2015).
[3]F. Deschler, M. Price, S. Pathak, L. E. Klintberg, D. D. Jarausch, R. Higler, S. Huttner, T. Leijtens, S. D. Stranks, H. J. Snaith, M. Atature, R. T. Phillips, and R. H. Friend, J. Phys. Chem. Lett. **5**, 1421 (2014).
[4]G. C. Xing, N. Mathews, S. S. Lim, N. Yantara, X. F. Liu, D. Sabba, M. Gratzel, S. Mhaisalkar, and T. C. Sum, Nat. Mater. **13**, 476 (2014).
[5]Z. K. Tan, R. S. Moghaddam, M. L. Lai, P. Docampo, R. Higler, F. Deschler, M. Price, A. Sadhanala, L. M. Pazos, D. Credgington, F. Hanusch, T. Bein, H. J. Snaith, and R. H. Friend, Nat. Nanotechnol. **9**, 687 (2014).
[6]B. R. Sutherland, S. Hoogland, M. M. Adachi, C. T. O. Wong, and E. H. Sargent, ACS Nano **8**, 10947 (2014).
[7]Q. Zhang, S. T. Ha, X. F. Liu, T. C. Sum, and Q. H. Xiong, Nano Lett. **14**, 5995 (2014).
[8]J. Even, L. Pedesseau, and C. Katan, J. Phys. Chem. C **118**, 11566 (2014).
[9]J. M. Frost, K. T. Butler, F. Brivio, C. H. Hendon, M. van Schilfgaarde, and A. Walsh, Nano Lett. **14**, 2584 (2014).
[10]M. Saba, M. Cadelano, D. Marongiu, F. Chen, V. Sarritzu, N. Sestu, C. Figus, M. Aresti, R. Piras, A. G. Lehmann, C. Cannas, A. Musinu, F. Quochi, A. Mura, and G. Bongiovanni, Nat. Commun. **5**, 5049 (2014).

[11]K. Wu, A. Bera, C. Ma, Y. Du, Y. Yang, L. Li, and T. Wu, Phys. Chem. Chem. Phys. **16**, 22476 (2014).
[12]Y. Yamada, T. Nakamura, M. Endo, A. Wakamiya, and Y. Kanemitsu, J. Am. Chem. Soc. **136**, 11610 (2014).
[13]T. J. Savenije, C. S. Ponseca, L. Kunneman, M. Abdellah, K. Zheng, Y. Tian, Q. Zhu, S. E. Canton, I. G. Scheblykin, T. Pullerits, A. Yartsev, and V. Sundström, J. Phys. Chem. Lett. **5**, 2189 (2014).
[14]T. C. Sum and N. Mathews, Energy Environ. Sci. **7**, 2518 (2014).
[15]S. Y. Sun, T. Salim, N. Mathews, M. Duchamp, C. Boothroyd, G. C. Xing, T. C. Sum, and Y. M. Lam, Energy Environ. Sci. **7**, 399 (2014).
[16]I. B. Koutselas, L. Ducasse, and G. C. Papavassiliou, J. Phys.: Condens. Matter **8**, 1217 (1996).
[17]K. Tanaka, T. Takahashi, T. Ban, T. Kondo, K. Uchida, and N. Miura, Solid State Commun. **127**, 619 (2003).
[18]Q. Lin, A. Armin, R. C. R. Nagiri, P. L. Burn, and P. Meredith, Nat. Photonics **9**, 106 (2015).
[19]A. Miyata, A. Mitioglu, P. Plochocka, O. Portugall, J. T.-W. Wang, S. D. Stranks, H. J. Snaith, and R. J. Nicholas, Nat. Phys. **11**, 582 (2015).
[20]Y. Yamada, T. Nakamura, M. Endo, A. Wakamiya, and Y. Kanemitsu, IEEE J. Photovoltaics **5**, 401 (2015).
[21]J. Kalinowski, M. Cocchi, D. Virgili, and C. Sabatini, Appl. Phys. Lett. **89**, 011105 (2006).
[22]H. Najafov, I. Biaggio, T.-K. Chuang, and M. Hatalis, Phys. Rev. B **73**, 125202 (2006).
[23]J. Pedrós, Y. Takagaki, T. Ive, M. Ramsteiner, O. Brandt, U. Jahn, K. Ploog, and F. Calle, Phys. Rev. B **75**, 115305 (2007).
[24]A. D. Mohite, P. Gopinath, H. M. Shah, and B. W. Alphenaar, Nano Lett. **8**, 142 (2008).
[25]C. Klingshirn, *Semiconductor Optics* (Springer, 2007).
[26]M. Samiee, S. Konduri, B. Ganapathy, R. Kottokkaran, H. A. Abbas, A. Kitahara, P. Joshi, L. Zhang, M. Noack, and V. Dalal, Appl. Phys. Lett. **105**, 153502 (2014).
[27]H. Zhu, Y. Fu, F. Meng, X. Wu, Z. Gong, Q. Ding, M. V. Gustafsson, M. T. Trinh, S. Jin, and X. Y. Zhu, Nat. Mater. **14**, 636 (2015).
[28]D. M. Bagnall, Y. F. Chen, Z. Zhu, T. Yao, M. Y. Shen, and T. Goto, Appl. Phys. Lett. **73**, 1038 (1998).
[29]X. H. Zhang, S. J. Chua, A. M. Yong, H. D. Li, S. F. Yu, and S. P. Lau, Appl. Phys. Lett. **88**, 191112 (2006).
[30]S. M. Sze and K. K. Ng, *Physics of Semiconductor Devices* (John Wiley & Sons, New York, 1981).
[31]B. Zhang, Y. Hou, F. Teng, Z. Lou, X. Liu, and Y. Wang, Appl. Phys. Lett. **96**, 103303 (2010).
[32]Z. D. Popovic, M. I. Khan, A. M. Hor, J. L. Goodman, and J. F. Graham, J. Phys. Chem. B **106**, 8625 (2002).
[33]J. Kalinowski, W. Stampor, J. Mężyk, M. Cocchi, D. Virgili, V. Fattori, and P. Di Marco, Phys. Rev. B **66**, 235321 (2002).
[34]D. F. Blossey, Phys. Rev. B **2**, 3976 (1970).
[35]D. F. Blossey, Phys. Rev. B **3**, 1382 (1971).
[36]D. A. B. Miller, D. S. Chemla, and S. Schmittrink, Phys. Rev. B **33**, 6976 (1986).